

# OPTIMAL SHAPE AND INCLUSION

## *open problems*

J.-M. Chassery<sup>1</sup> and D. Coeurjolly<sup>2</sup>

<sup>1</sup>*Laboratoire LIS, CNRS UMR 5083  
961, rue de la Houille Blanche - BP46,  
F-38402 St Martin d'Hères, France  
Jean-marc.Chassery@lis.inpg.fr*

<sup>2</sup>*Laboratoire LIRIS, CNRS FRE 2672  
Universite Claude Bernard Lyon 1,  
43, Bd du 11 novembre 1918,  
F-69622 Villeurbanne, France  
david.coeurjolly@liris.cnrs.fr*

**Abstract** Access to the shape by its exterior is solved using convex hull. Many algorithms have been proposed in that way. This contribution addresses the open problem of the access of the shape by its interior also called convex skull. More precisely, we present approaches in discrete case. Furthermore, a simple algorithm to approximate the maximum convex subset of star-shaped polygons is described.

**Keywords:** shape approximation, convex hull, convex skull, potato peeling.

## **Introduction**

In digital image processing we are often concerned with developing specialized algorithms that are dealing with the manipulation of shapes. A very classical and widely studied approach is the computation of the convex hull of an object. However, most of these studies focus only on exterior approaches for the computation of convexity, i.e., they are looking for the smallest convex set of points including a given shape. This contribution addresses the problem of the access of the shape by its interior. The computation of the best shape according to a criterion included in a given one has been studied in many few occasions in the continuous case involving convex skull and potato peeling.

In this article, we present successive configurations of fast approximation of the maximal convex subset of a polygon. First a discrete approach will illustrate an iterative process based on shrinking and convex hull. Second a

region based approach will be proposed in specific case where the criterion is maximal horizontal-vertical convexity. Third study will be focused to the family of star-shaped polygons  $P$ . A simple algorithm extracts the maximal convex subset in  $O(k \cdot n)$  in the worst case if  $n$  is the size of  $P$  and  $k$  its number of reflex points.

In section 1, we list classical problems of shape approximation. In section 2, we present the discrete approach followed by h-v convexity in section 3. In section 4, we introduce the Chang and Yap's optimal solution definitions that will be used in the rest of the presentation. In section 5, we present the proposed algorithm based on classical and simple geometric tools for star-shaped polygons. Finally, experiments are given.

## 1. Shape approximations

In this paper shapes are delimited by polygonal boundary. We suppose that polygons are simple in the sense that they are self-avoiding. Polygon inclusion problems are defined as follows: given a non-convex polygon, how to extract the maximum area subset included in that polygon ? In [7], Goodman calls this problem the *potato-peeling problem*. More generally, Chang and Yap [3] define the polygon *inclusion* problem class  $Inc(\mathcal{P}, \mathcal{Q}, \mu)$ : given a general polygon  $P \in \mathcal{P}$ , find the  $\mu$ -largest  $Q \in \mathcal{Q}$  contained in  $P$ , where  $\mathcal{P}$  is a family of polygons,  $\mathcal{Q}$  the set of solutions and  $\mu$  a real function on  $\mathcal{Q}$  elements such that

$$\forall Q' \in \mathcal{Q}, \quad Q' \subseteq Q \Rightarrow \mu(Q') \leq \mu(Q). \quad (1)$$

The maximum area convex subset is an inclusion problem where  $\mathcal{Q}$  is the family of convex sets and  $\mu$  gives the area of a solution  $Q$  in  $\mathcal{Q}$ . The inclusion problem arises in many applications where a quick internal approximation of the shape is needed [2, 5].

In a dual concept, we can mention enclosure problem presented as follows: given a non-convex polygon, how to extract the minimum area subset including that polygon ? We can define the polygon *enclosure* problem class  $Enc(\mathcal{P}, \mathcal{Q}, \mu)$ : given a general polygon  $P \in \mathcal{P}$ , find the  $\mu$ -smallest  $Q \in \mathcal{Q}$  containing  $P$ , where  $\mathcal{P}$  is a family of polygons,  $\mathcal{Q}$  the set of solutions and  $\mu$  a real function on  $\mathcal{Q}$  elements such that

$$\forall Q' \in \mathcal{Q}, \quad Q' \supseteq Q \Rightarrow \mu(Q') \geq \mu(Q). \quad (2)$$

### 1.1 Examples

The following list corresponds to examples of various situations depending on specifications of the  $\mathcal{P}$  family, the  $\mathcal{Q}$  family and the  $\mu$  measure.

**Example 1.**  $\mathcal{P}$  is a family of simple polygons,

$\mathcal{Q}$  is the family of convex polygons,  
 $\mu$  is the area measure,  
 $Enc(\mathcal{P}, \mathcal{Q}, \mu)$  is the problem of convex hull

**Example 2.**  $\mathcal{P}$  is a family of simple polygons,  
 $\mathcal{Q}$  is the family of convex polygons,  
 $\mu$  is the area measure,  
 $Inc(\mathcal{P}, \mathcal{Q}, \mu)$  is the problem of potatoe peeling [7, 3]

**Example 3.**  $\mathcal{P}$  is a family of n-sided convex polygons,  
 $\mathcal{Q}$  is the family of triangles,  
 $\mu$  is the area measure,  
 $Inc(\mathcal{P}, \mathcal{Q}, \mu)$  has a solution with complexity in  $O(n)$

**Example 4.** [9]  $\mathcal{P}$  is a family of n-sided simple polygons,  
 $\mathcal{Q}$  is the family of triangles,  
 $\mu$  is the area measure,  
 $Enc(\mathcal{P}, \mathcal{Q}, \mu)$  has a solution with complexity in  $O(n \log^2 n)$   $O(n \log^2 n)$

**Example 5.** [8]  $\mathcal{P}$  is a family of n-sided simple polygons,  
 $\mathcal{Q}$  is the family of rectangles,  
 $\mu$  is the area measure,  
 $Enc(\mathcal{P}, \mathcal{Q}, \mu)$  has a solution with complexity in  $O(n)$  in 2D,  $O(n^3)$  in 3D.

**Example 6.**  $\mathcal{P}$  is a family of n-sided orthogonal polygons,  
 $\mathcal{Q}$  is the family of convex orthogonal polygons,  
 $\mu$  is the area measure,  
 $Inc(\mathcal{P}, \mathcal{Q}, \mu)$  has a solution with complexity in  $O(n^2)$  [12].  
 In the following we will focus on the problem 2.

## 2. Discrete approach

Let us consider a discrete shape defined as a connected set of pixels. The objective is to find a maximal convex set included in that discrete shape [4] .

The proposed algorithm is iterative, starting from the initial shape. Each iteration is composed of a shrinking and computation of the convex hull of the shrunked shape. If the convex hull is not included in the initial shape, we reiterate the shrinking process. Else we detect the side of the convex hull which contains concavity vertex of the initial connected component. We cut the initial component along this side and restart the algorithm with this new shape for initialization. The algorithm stops when the modified initial shape is convex. Figure 1 illustrates the different steps of this algorithm.

Figure 2 illustrates the result of this algorithm on various examples.

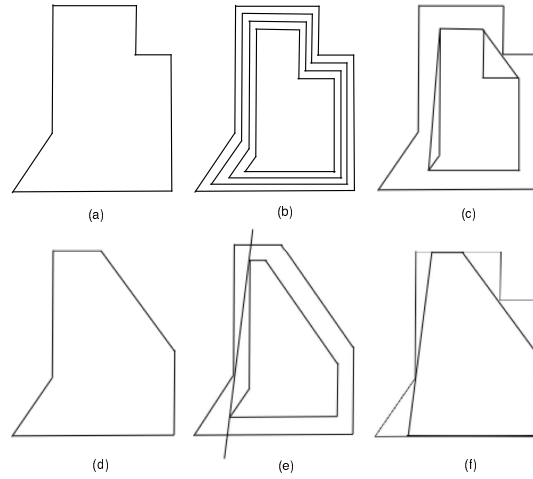


*Figure 1.* Iterative process by shrinking and convex hull computation: (a) initial shape, (b) successive shrinking, (c) the convex hull of the shrunk object is included in the initial shape, (d) cut of the initial shape for a second pass, (e) the convex hull of the shrunk object is included in the initial shape, (f) maximal solution.

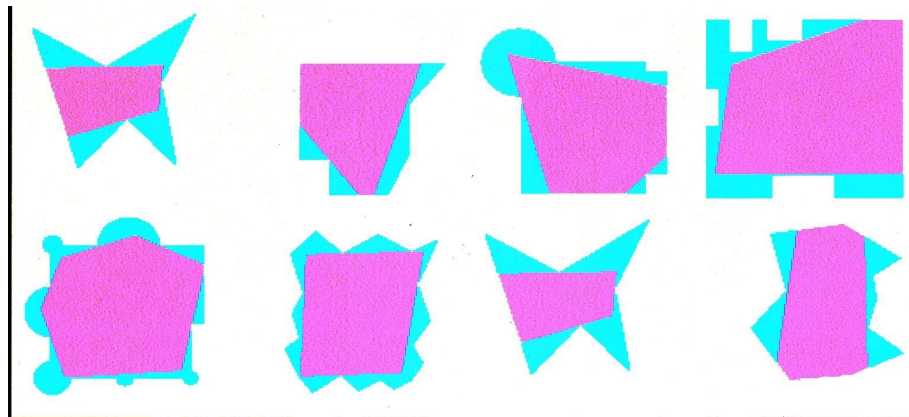


*Figure 2.* Illustration on different shapes: initial shape and result are superimposed.

In that case the  $\mu$  measure is not the area but the Min-max distance between the boundaries of the initial shape and the solution. This corresponds to the Hausdorff distance between the two shapes P and Q.

$$\mu(P, Q) = - \max(\sup_{M \in P} \inf_{N \in Q} d(M, N), \sup_{M \in Q} \inf_{N \in P} d(M, N))$$

where  $d$  is the digital distance based on 4 or 8 connectivity.

### 3. Limitation to h-v convexity

In that section we limit our study to the particular case of horizontal-vertical convexity noted by h-v convexity and illustrated on figure 3.

The search of the maximum ortho-convex polygon included into a simple orthogonal polygon has been solved in the continuous case by Wood and Yap with complexity in  $O(n^2)$  [12].

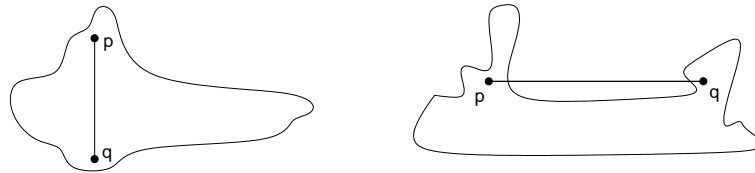


Figure 3. h-v convexity: In left the shape is h-v convex, in right the shape is not h-v convex..

We will briefly present a method in the discrete case. This work is issued from an Erasmus project and a detailed version is in the students' report (see <http://www.suerge.de/s/about/shape/shape.ps.gz>).

Let us consider a given shape as a set of 4-connected component . The principle of this method is to assign a weight to all the pixels in the shape and then to partition the shape into h-v convex regions according to these weights.

Basically, the entire process consists of four steps which are: - *Horizontal/Vertical Sweeping for weight assignement* and - *Labeling of the shape into regions* and - *Construction of Adjacency and Incompatibility graphs between the labeled regions* and - *Finding the solution(s)*.

Illustration of these steps is given on the following example.

The weight being attached to each shape pixel indicates the number of sections (h-section and v-section) that include this pixel. The minimum weight of any shape pixel is equal to two. Figure 4 illustrates the weights assignation.

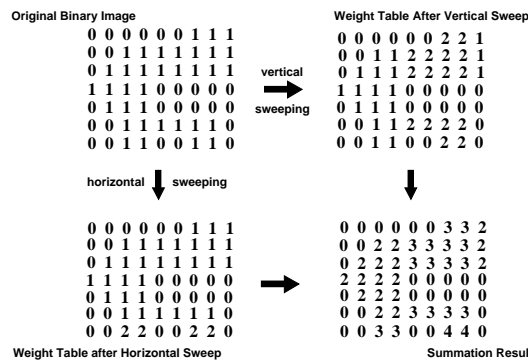


Figure 4. Examples that simulate how the weights are being assigned.

A region is a maximal connected set of pixels having the same weight. The labeling process provides a different label to each region. It needs two steps:

1. Extract all the pixels with a same weight and generate a weighted image.
2. Perform labeling on this weighted image.

These two steps will be performed iteratively until all the different weights have been labeled (figure 5).

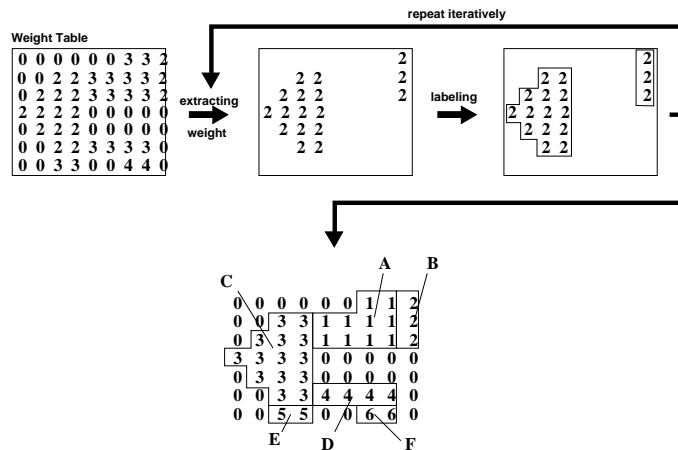


Figure 5. An example that illustrates the labeling process.

Next step will illustrate relationships between regions in term of coexistence in a hv-convex set. Two graphs are introduced in which regions are vertices: Adjacency Graph and Incompatibility Graph.

The Adjacency Graph defines the connectivity between the different regions. It indicates that they can be merged to find the biggest hv-convex set. Two regions are adjacent to each other and their respective nodes will be linked if there is at least one pixel of each region neighbouring each other (figure 6).

The Incompatibility Graph defines the confliction between different regions. It indicates that they cannot be combined at the same time to find the biggest hv-convex set. Two regions are conflicting with each other and their respective nodes will be linked if there is at least one pixel of each region separated from each other by a h-section (or v-section) of background pixels (figure 6).

Before starting the graphs analysis we have to realise that every region is a solution, since every region is hv-convex itself and is included in the shape. However finding just a solution is not sufficient, since we are interested in the maximum or even optimal solution. A maximum solution is a solution in which no other region can be added without violating the hv-convexity constraint. The optimum solution is the best possible maximum solution. It does not have to be unique. To find the best solution we have to determine all the maximum solutions issued from the following steps.

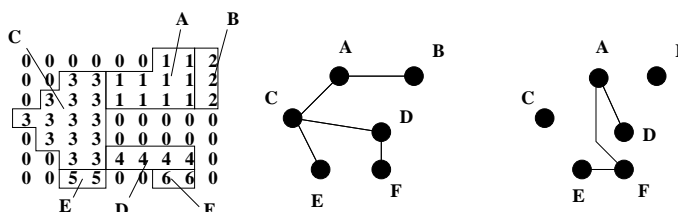


Figure 6. Adjacency (middle) and Incompatibility (right) graphs from the labeled shape (left).

1. Pick a region and put this in an initially empty set (let us call this set A).
2. Construct two lists, one called the adjacency list and the other one called the incompatibility list. These lists contain the labels of the regions which are respectively adjacent and conflicting with the regions in set A. If there is a region, which is in the adjacency list (and not in the incompatibility list), then add this to set A and update both lists. When this cannot be done anymore, we have found a maximum solution, since we do not have anymore candidates on the adjacency list.
3. Backtrack is needed to solve the problem of choice in the adjacency list. A region, which has not been picked before, should be placed into set A.
4. At the moment that all possibilities have been tried, we can change the initial region with which we started the search and go back to step 2 until every region has been the initial region of the set A.

If at every step the current solution is compared with the best solution so far, then at the end of the algorithm one of the optimal solutions is found.

The illustration in figure 7 shows the construction of maximal solutions by traversing the graphs of adjacency and incompatibility.

#### 4. Preliminaries and Exact Polynomial Solution

For the rest of the presentation, we consider a polygon  $P = (v_0, v_1, \dots, v_{n-1})$  with  $n$  vertices. We denote by  $R = (r_0, r_1, \dots, r_{k-1})$  the  $k$  reflex vertices (or concave vertices) of  $P$  (maybe empty). The potato-peeling problem can be expressed as follows,

PROBLEM 1 Find the maximum area convex subset (MACS for short)  $Q$  contained in  $P$ .

- In [7], Goodman proves that  $Q$  is a convex polygon. He presents explicit solutions for  $n \leq 5$  and leaves the problem unsolved in the general case.
- In [3], Chang and Yap prove that the potato-peeling problem can be solved in polynomial time in the general case. More precisely, they detail an  $O(n^7)$  time algorithm to extract  $Q$  from  $P$ . Since this algorithm uses complex geometric

Possible Solutions	Adjecency List	Incompatibility List
A	B C	D F
A B	C	D F
A B C	E	D F
A B C E ← Maximum Solution		D F
A C	B E	D F
A B C	E	D F
A B C E ← Maximum Solution		D F
A C E	B	D F
A B C E ← Maximum Solution		D F
. . . .	.	. .
C	A D E	
C D	E F	A
C D E ← Maximum Solution		A F
C D F ← Maximum Solution		A E
C A	B E	D F
C A B	E	D F
C A B E ← Maximum Solution		D F
. . . .	.	. .

Figure 7. Table showing how to traverse the graphs of adjacency and incompatibility to get maximal solutions. ABCE is the optimal solution.

concepts and dynamic programming in several key steps, it is not tractable in practical applications.

Let us present some elements of the Chang and Yap's algorithm. First of all, we define a *chord* of  $P$  by a maximal segment fully contained in  $P$ . A chord is said to be *extremal* if it contains two or more vertices of  $P$ . In particular, an edge of  $P$  is always enclosed in an extremal chord. Let  $C_1, C_2, \dots, C_m$  be chords of  $P$  with  $m \leq k$  such that each  $C_i$  passing through reflex vertices of  $P$ . We first consider the chords going through a unique reflex point. Let us associate to each such a chord  $C_i$  passing through  $u$  in  $R$ , the closed half-plane  $C_i^+$  defined by  $C_i$  and such that at least one or two adjacent vertices to  $u$  does not belong to  $C_i^+$ . If  $C_i$  passes through more than one reflex vertex, the choice of the half-plane can be made in similar ways (see figure 8). They prove that the maximum area convex polygon  $Q$  is given by the intersection of  $P$  and a set of half-planes defined by a set of so-called optimal chords (see [3]). Hence, to solve the potato-peeling problem, we have to find the appropriate set of optimal chords associated to the reflex vertices.

If  $P$  has only one reflex vertex  $u$ , the optimal chord  $C_u$  that leads to the MACS  $Q$  can be easily found. First of all, Chang and Yap [3] define a *butterfly* as a sequence of points  $[b', a, u, b, a']$  such that  $a, u$  and  $b$  are consecutive vertices in  $P$  with  $a$  and  $b$  adjacent vertices of  $u$  in  $P$ , and such that both  $[a, u, a']$  and  $[b, u, b']$  are extremal chords (see figure 9). Furthermore, the chord  $[c, u, c']$  is said to be *balanced* if we have  $|cu| = |uc'|$  ( $c$  and  $c'$  belonging to  $P$ ). Based

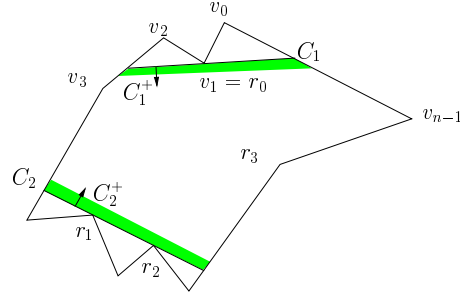


Figure 8. Notations and illustrations of chords and half-planes generated by these chords.

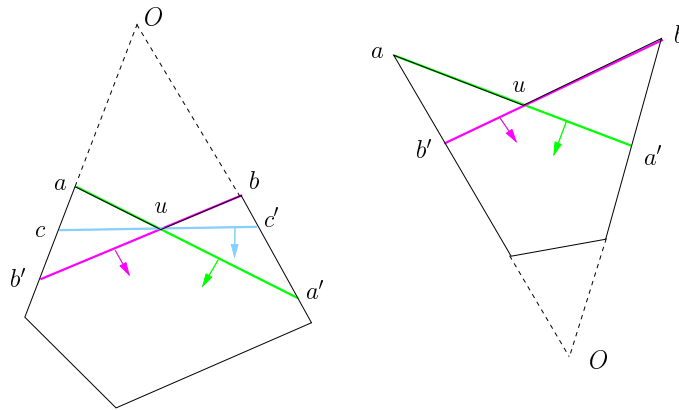


Figure 9. One reflex vertex case: an A-butterfly (left) and a V-butterfly (right). According to lemma 2, the optimal chord of each polygon is one of the gray segments.

on these definitions, two kinds of butterflies exist according to the position of the intersection  $O$  between the straight lines  $(b'a)$  and  $(ba')$ , and the polygon. More precisely, a *A-butterfly* is such that the points  $b', a$  and  $O$  (or  $O, b$  and  $a'$ ) appear in this order (see figure 9-(left)) in the straight line  $(ab)$  (resp.  $(a'b')$ ). Otherwise, it is called a *V-butterfly* (see figure 9-(right)). In this one reflex corner case, Chang and Yap prove the following lemma:

LEMMA 2 (BUTTERFLY LEMMA [3]) *Given a butterfly  $B$  and its optimal chord  $C_u$ , if  $B$  is a V-butterfly then  $C_u$  is an extremal chord. If  $B$  is a A-butterfly,  $C_u$  is either extremal or balanced.*

We notice that in case of V-butterfly we have two possible chords, in case of A-butterfly, three choices are possible. This lemma leads to a linear in time solution to the potato-peeling problem if  $k = 1$ .

In a general case, Chang and Yap [3] define other geometric objects such as series of A- and V-butterflies. Based on these definitions, they present an

A-lemma and a V-lemma, similar to lemma 2, that state that the optimal chords for a set of butterflies are extremal chords or a set of balanced chords. In the general case, the definition of a balanced chain for a butterfly sequence is more complex than in the previous case (see figure 10-(a)). Hence, the computation of such a chain uses dynamic programming and complex geometric concepts. Furthermore this step is the bottleneck of the algorithm and makes expensive the  $O(n^7)$  global time complexity.

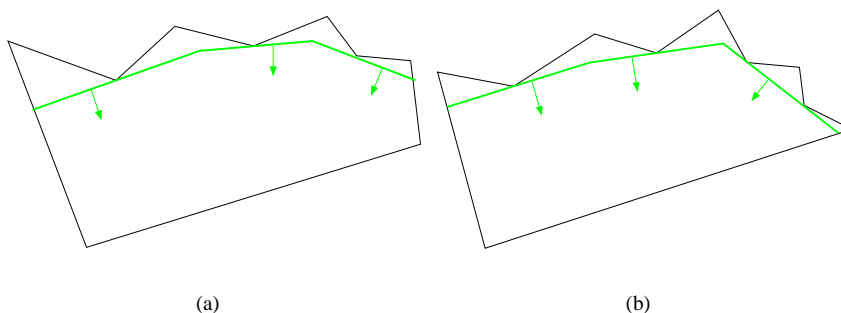


Figure 10. Examples of balanced chains of A-butterflies series: (a) a balanced chain given by single-pivot chords and (b) given by both single- and double-pivot chords.

To end with definitions, Chang and Yap divide the set of balanced chords into two classes: a balanced chord is called *single-pivot* if it contains only one reflex vertex (chord  $C_1$  in figure 8) and *double-pivot* if it contains two distinct reflex points (chord  $C_2$  in figure 8). Finally, the optimal set of chords that defines the MACS of  $P$  contains extremal, balanced single-pivot and balanced double-pivot chords. In figure 10-(a), the solution is composed by only single-pivot chords, in figure 10-(b) both single- and double-pivot chords. Note that for a reflex vertex  $r_i$ , from the set of extremal chords associated to  $r_i$ , we just have to consider the two extremal chords induced by the two adjacent edges to  $r_i$ . In the following, we restrict the definition of an extremal chord to a chord that contains an edge of  $P$  incident to a reflex vertex.

Our contribution starts here. In the next section, we present a fast algorithm to approximate the maximum area convex subset star-shaped polygons that uses Chang and Yap's analysis.

## 5. Fast approximation algorithm

### 5.1 Kernel dilatation based heuristic

In this section, we assume that  $P$  is a star-shaped polygon. First of all, we remind basic definitions of such a polygon.  $P$  is a *star-shaped polygon* if there exist a point  $q$  in  $P$  such that  $q\bar{v}_i$  lies inside  $P$  for all vertices  $v_i$  of  $P$ . The set

of points  $q$  satisfying this property is called the *kernel* of  $P$  [11]. Using our definitions and [11], we have:

**PROPOSITION 3** *The kernel of  $P$  is given by the intersection between  $P$  and the half-planes  $C_i^+$  defined by all extremal chords  $C_i$  associated to all reflex vertices.*

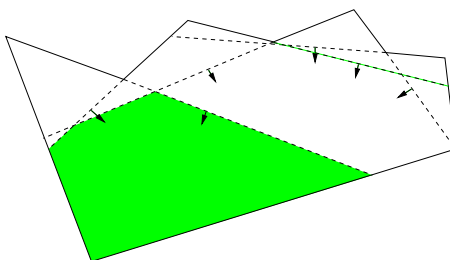


Figure 11. Illustration of the kernel computation of the example in figure 10-(a).

Figure 11 is an illustration of such proposition. We have the theorem.

**THEOREM 4** *Let  $P$  be a star-shaped polygon, then its kernel is a subset of the maximum area convex subset of  $P$ .*

**PROOF.** Let  $C_i$  be the optimal chord associated to a reflex point  $r_i$  of  $P$ . We consider the closed space  $K$  defined by the intersection between  $P$  and the two extremal chords of  $r_i$ . If  $C_i$  is an extremal chord, it is clear that  $K \subseteq (C_i^+ \cap P)$ . If  $C_i$  is a single or double-pivot balanced chord, the slope of  $C_i$  is strictly bounded by the slopes of the two extremal chords. Furthermore, since all the half-planes have the same orientation according to  $P$  and  $r_i$ , we also have  $K \subseteq (C_i^+ \cap P)$  (see figure 9-(left) for example). Finally, since the maximum area convex polygon is the intersection between  $P$  and the set of half-planes defined by optimal chords, and since the two extremal chords always define a subset to the associated optimal chord, the intersection of all extremal chords is a subset of the MACS of  $P$ . With proposition 3, the kernel of  $P$  is a convex subset of the MACS.  $\square$

In other words, there exists a continuous deformation that transforms the kernel to the MACS. In the following, the strategy we choose to approximate the MACS is to consider the deformation as an Euclidean dilatation of the kernel. Based on this heuristic, several observations can be made: the reflex vertices must be taken into account in the order in which they are reached by the dilatation wavefront. More formally, we consider the list  $\mathcal{O}$  of reflex vertices such that the points are sorted according to their minimum distance

to the kernel polygon. When a reflex vertex is analyzed, we fix the possible chords and introduce new definitions of chords as follows:

- the chord may be an extremal one as defined by Chang and Yap;
- the chord may be a single-pivot chord such that its slope is tangent to the wavefront (this point will be detailed in the next section);
- the chord may be a double-pivot chord. In that case, the second reflex vertex that belongs to the chord is necessary. It must correspond to the next reflex point in the order  $\mathcal{O}$ .

Furthermore, when a reflex vertex is analyzed, we choose the chord from this list that maximizes the area of the resulting polygon. If we denote by  $P'$  the polygon given by the intersection between  $P$  and the half-plane associated to the chosen chord, the chord must maximize the area of  $P'$ . In the algorithm, it is equivalent to minimize the area of the removed parts  $P/P'$ . Using these heuristics, the approximated MACS algorithm can be easily designed in a greedy process:

- 
- 1: Compute the kernel of  $P$
  - 2: Compute the ordered list  $\mathcal{O}$  of reflex vertices
  - 3: Extract the first point  $r_1$  in  $\mathcal{O}$
  - 4: **while**  $\mathcal{O}$  is not empty **do**
  - 5:   Extract the first point  $r_2$  in  $\mathcal{O}$
  - 6:   Choose the best chord that maximizes the resulting polygon area with the chords  $(r_1, r_2)$
  - 7:   Modify the polygon  $P$  accordingly
  - 8:   Update the list  $\mathcal{O}$  removing reflex points excluded by the chord
  - 9:    $r_1 \leftarrow r_2$
  - 10: **end while**
- 

## 5.2 Algorithms and complexity analysis

In this section, we detail the algorithms and their computational costs. Keep in mind that  $n$  denotes the number of vertices of  $P$  and  $k$  the number of reflex vertices.

**Distance-to-kernel computation.** First of all, the kernel of a polygon can be constructed in  $O(n)$  time using the Preparata and Shamos's algorithm [11]. Note that the number of edges of the kernel is  $O(k)$  (intersection of  $2k$  half-planes). The problem is now to compute the distances between the reflex vertices and the kernel of  $P$  denoted  $Kern(P)$ . A first solution is given by the

Edelsbrunner's algorithm that computes the extreme distances between two convex polygons [6].

However, we use another geometrical tool that will be reused in the next section. Let us consider the generalized Voronoi diagram of  $Kern(P)$  [11, 1]. More precisely, we are interested in the exterior part to  $Kern(P)$  of the diagram (see figure 12). As  $Kern(P)$  is convex, such a diagram is defined by exterior angular bisectors  $\{b_i\}_{i=1..5}$  of the kernel vertices. For example in figure 12, all exterior points to  $Kern(P)$  located between the angular bisectors  $b_0$  and  $b_1$ , are closer to the edge  $e$  (extremities are included) than to all other edges of  $Kern(P)$ . Hence, the minimum distance between such a point and  $Kern(P)$  is equal to the distance between the point and the edge  $e$ .

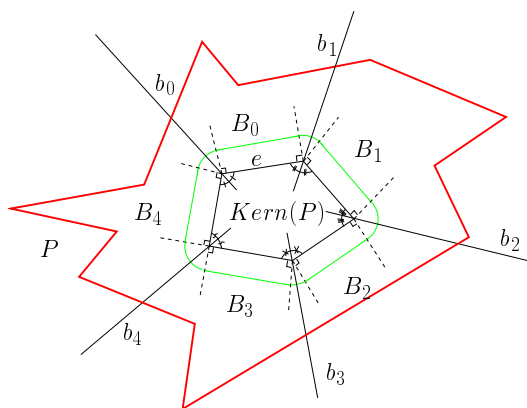


Figure 12. Euclidean growth of a convex polygon.

To efficiently compute the distance between all reflex vertices to the kernel, we first detail some notations. Let  $B_m$  be the open space defined by  $Kern(P)$  and the exterior angular bisectors  $b_m$  and  $b_{m+1}$  (if  $m+1$  is equal to  $|Kern(P)|$  then  $b_0$  is considered). Hence, the distance to kernel computation step can be viewed as a labelling of vertices of  $P$  according to the cell  $B_m$  they belong to. To solve this labelling problem, we have the following proposition.

**PROPOSITION 5** *The vertices of  $P$  that belong to the cell  $B_m$  form only one connected piece of  $P$ .*

**PROOF.** Let us consider an half-line starting at a point of  $Kern(P)$ . By definition of  $Kern(P)$ , the intersection between such an half-line and  $P$  is either a point or an edge of  $P$ . The special case when the intersection is an edge of  $P$  only occurs when the starting point belongs to an edge of  $Kern(P)$  and when the half-line is parallel to this edge (and thus parallel to an extremal chord of a reflex vertex of  $P$ ). Hence, using the definition of the exterior angular bisectors and given a cell  $B_m$ , the

half-line  $b_m$  (resp.  $b_{m+1}$ ) crosses  $P$  at a point  $p_m$  (resp.  $p_{m+1}$ ) of  $P$ . Furthermore, each vertex of  $P$  between  $p_m$  and  $p_{m+1}$  belongs to  $B_m$ , otherwise the number of intersections between  $P$  and  $b_m$  or  $b_{m+1}$  should be greater than one. Finally, only one connected piece of  $P$  belongs to  $B_m$ .  $\square$

Then the proposition implies the corollary:

**COROLLARY 6** *The order of the  $P$  vertex labels is given by the edges of  $Kern(P)$ .*

Hence, we can scan both the vertices of  $P$  and the edges of  $Kern(P)$  to compute the distance-to-kernel. We obtain the following simple algorithm<sup>1</sup>:

---

```

1: Find the closest edge  $e_j$  of  $Kern(P)$  to the point  $v_0 \in P$ 
2: for  $i$  from 1 to  $n$  do
3:   while  $d(v_i, e_j) > d(v_i, e_{j+1 \pmod{|Kern(P)|}})$  do
4:      $j := j + 1 \pmod{|Kern(P)|}$ 
5:   end while
6:   Store the distance  $d(v_i, e_j)$  to  $v_i$ 
7: end for

```

---

To detail the computational costs, the step 1 of this algorithm is done in  $O(k)$  and the cost of the **For** loop is  $O(n)$ . As the matter of fact, using Prop. 5 and excepted for the first edge  $e_j \in Kern(P)$  of step 1, when we go from an edge  $e_{j'}$  to next one, the piece of  $P$  associated to the cell  $B_m$  defined by  $e_{j'}$  is completely computed. Hence, each edge of  $Kern(P)$  is visited once during all the process. Note that the first edge  $e_j$  of step 1 may be used twice to complete the scan of  $P$ .

Finally, the minimum distances between the vertices of  $P$  and  $Kern(P)$  are computed in  $O(n)$ . Note that since we are only interested in labelling reflex vertices, the above algorithm can be transformed to have a  $O(k)$  computational cost. However, a  $O(n)$  scanning of  $P$  is still needed to identify reflex points. Furthermore, the sorted list  $\mathcal{O}$  of reflex points according to such distance is computed in  $O(k \cdot \log k)$ .

**Single-pivot chords computation.** Given a reflex point  $r_i$  of  $P$ , we have listed three possible classes of chord: extremal, single-pivot and double-pivot chords. The figure 13 reminds the possible chords. The extremal and double-pivot chord computation is direct. However, we have to detail the single-pivot chord extraction. According to our heuristic, the single-pivot chord associated to  $r_i$  must be tangent to the wavefront propagation of the kernel dilatation.

Using the exterior angular bisector structure we have introduced above, we can efficiently compute the slopes of such chords. In figure 14-(a), let  $e_1$  and

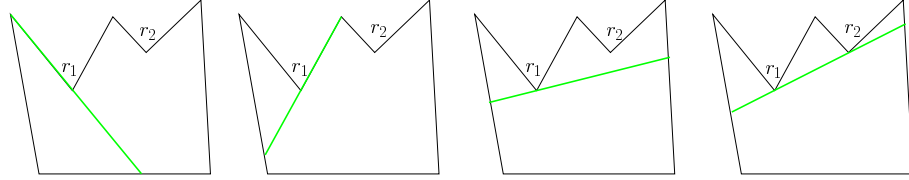


Figure 13. All possible chords that can be associated to the reflex point  $r_1$  (the two extremal chords, a single-pivot balanced chord and the double-pivot chord).

$e_2$  be two adjacent edges of  $Kern(P)$  ( $e_1$  and  $e_2$  are incident to the vertex  $v$ ). Let  $p$  (resp.  $q$ ) be a point in the plane that belongs to the cell generated by  $e_1$  (resp.  $e_2$ ). We can distinguish two cases:  $p$  is closer to  $e_1$  than to one of its extremities and  $q$  is closer to  $v$  than to  $e_2$  (without the extremities). Hence the straight line going through  $p$  and tangent to the wave-front propagation is parallel to  $e_1$ . In the second case, the tangent to wavefront straight line going through  $q$  is tangent to the circle of center  $v$  and radius  $\|vq\|$  (see figure 14). Moreover, two particular cases can be identified (see figure 14-(b)): the first one occurs when the distance between  $v$  and  $q$  is null, in that case the slope of the chord is the mean of the slopes of edges  $e_1$  and  $e_2$ . The second case occurs when the single-pivot chord does not fulfill the maximal chord definition (see the right figure in 14-(b)). In that case, we do not consider this single-pivot chord in the optimal chord choice of line 6 in the main algorithm. Note that this last particular case can also occur with double-pivot chords. In such cases, the chord is not considered too.

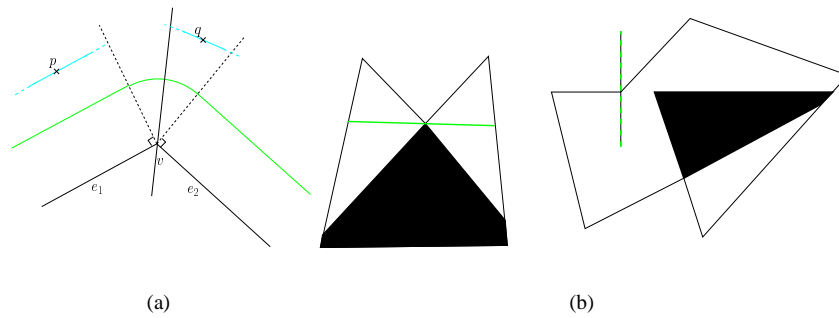


Figure 14. Computing a chord parallel to the kernel dilatation wavefront: (a) slope computation in the general case, (b) illustration of the two particular cases: the distance between the reflex point and the kernel is null and the single-pivot chord is not a maximal chord.

Finally, if each reflex point  $r_i$  of  $P$  is labelled according to the closest edge  $e_i$  of  $Kern(P)$  (extremities included), we can directly compute the single-

pivot chord: if  $r_i$  is closer to  $e_j$  than one of its extremities, the chord is parallel to  $e_j$ , otherwise, the chord is tangent to a given circle.

Note that this labelling can be obtained using the previous distance-to-kernel algorithm. Finally, the computation of the  $k$  single-pivot chords is done in  $O(k)$ .

**Polygon cut and area evaluation.** Given a reflex point  $r_i$  and a chord  $C_i$  either extremal, single-pivot or double-pivot, we have to compute the resulting polygon of the intersection between  $P$  and  $C_i^+$ . We suppose that the vertices of  $P$  are stored as a doubly-connected list.

The cutting algorithm is simple: starting from  $r_i$ , the vertices of  $P$  are scanned in the two directions until they belong to  $C_i^+$  (see figure 15).

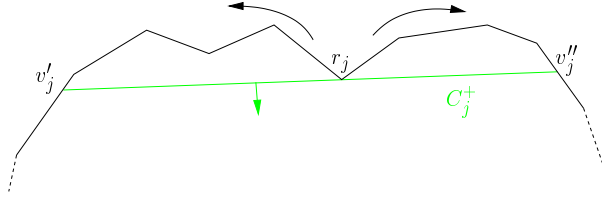


Figure 15. Illustration of the vertex scan to compute the  $(P \cap C_i^+)$  polygon.

During the process, let  $m$  be the number of removed vertices. Hence, the polygon cut according to  $C_i$  is done in  $O(m)$ . Furthermore, the resulting polygon has got  $n - m$  vertices. Hence, given  $k$  reflex vertices and  $k$  chords, the resulting polygon is computed in  $O(n)$ : each vertex is visited a constant number of times.

Furthermore, the area of the removed parts can be computed without changing the computational cost. Indeed, let  $p$  be a point in the plane, the area of a polygon  $P$  is given by

$$\mathcal{A}(P) = \frac{1}{2} \sum_{i=0}^{n-1} \mathcal{A}(p, v_i, v_{i+1 \pmod{n}}), \quad (3)$$

where  $\mathcal{A}(p, v_i, v_j)$  denotes the signed area of the triangle  $(p, v_i, v_j)$  [10]. Hence, the area can be computed in a greedy process during the vertex removal process.

### 5.3 Overall computational analysis

Based on the previous analyses, we can detail the computational cost of the global algorithm presented in the section 5.1. First of all, step 1 (kernel determination) requires  $O(n)$  computation using [11]. Then, we have presented a simple  $O(n)$  algorithm to compute the distance-to-kernel of reflex vertices and

thus the cost of step 2 (reflex vertices sorting) is  $O(n + k \cdot \log k)$ . The Step 3 and the step 5 in the **while** loop on reflex vertices requires  $O(1)$  computations.

Given the two reflex points  $r_1$  and  $r_2$  of step 6, we have to decide which chord should be associated to  $r_1$ . We have two extremal chords, a single-pivot chord whose slope is computed in  $O(1)$  and a double-pivot chord going through  $r_2$ . Using our heuristics, we choose the chord that minimizes the removed part of  $P$ . Hence, we compare the removed part area using the double chord and the 9 area measures of the  $3 \times 3$  other possible choices for  $r_1$  and  $r_2$ . Hence, at each step of the **while** loop, we compute 10 polygon cuts and we choose, for the  $r_1$  chord, the chord that maximizes the resulting polygon area. Note that steps 7 and 8 are computed during the polygon cutting steps and do not change the computational cost.

In the worst case, each polygon cut step is done in  $O(n)$ . Hence, the overall complexity of the **while** loop is  $O(k \cdot n)$ . Finally, the cost of the approximated MACS extraction algorithm is  $O(k \cdot n)$  in the worst case. Let  $N$  be the number of removed vertices while evaluating the optimal chord at  $r_1$  in step 6. If we suppose that the reflex vertices of  $P$  are *uniformly distributed* in the sense that each other tested chord only visits the same amount  $O(N)$  of vertices. Then, at each step,  $O(N)$  vertices are visited and the modified polygon has got  $O(n - N)$  vertices. Hence, the **while** loop complexity becomes  $O(n)$ . This leads to a global cost for the approximated MACS extraction in  $O(n + k \cdot \log k)$ . In practice, such *uniformity* has been observed in our examples.

To speed up the algorithm, several optimizations can be done without changing the worst case complexity. For example, when chords going through  $r_2$  are tested, the obtained polygons are propagated to the next step of the while loop in order to reduce the number of polygon cut steps. Furthermore, since the area of the removed parts is computed during the vertex scan, the process can be stopped if the area is greater than the current minimum area already computed with other chords.

## 5.4 Experiments

In this section, we present some results of the proposed algorithm. First of all, the figure 16 compares the results between the optimal Chang and Yap's algorithm [3] and the approximated MACS extraction process. In practical experiments, the optimal  $O(n^7)$  algorithm do not lead to a direct implementation. Indeed, many complex geometrical concepts are used and the overall algorithm is not really tractable. Hence, we use a doubly-exponential process to extract the optimal MACS. The main drawback of this implementation is that we cannot extract the optimal MACS if the number of the polygon points is important. In figure 16, the first column presents the polygon, its kernel and the distance labelling of all vertices, the second row contains the optimal

MACS and the third one the approximated MACS. Note that the results of the last row are identical.

If we compute the area error between the optimal and the approximated MACS on these examples, the error is less than one percent.

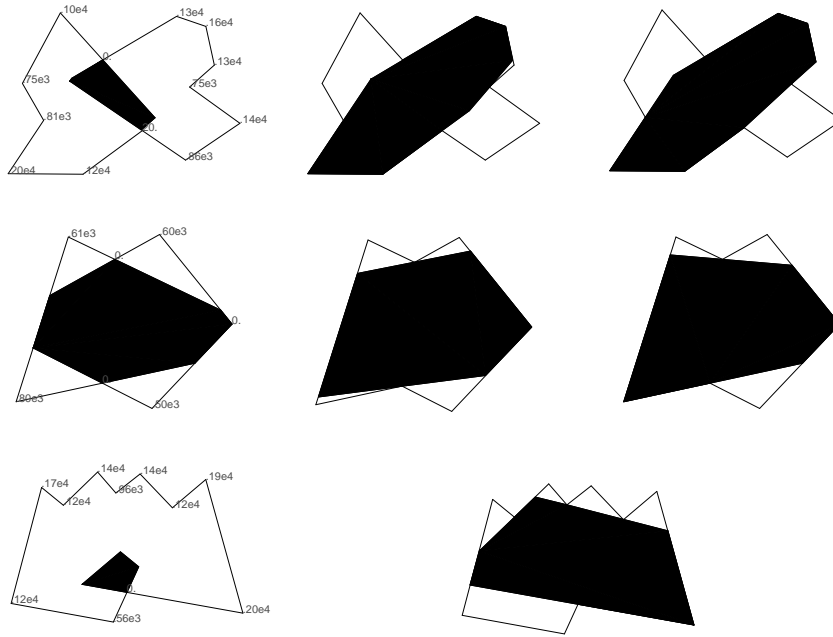


Figure 16. Comparisons between the optimal MACS and the proposed algorithm: the first column presents the input polygons, their kernels and the distance labelling, the second column shows the results of the Chang and Yap’s algorithm. The last row present the result of the proposed algorithm.

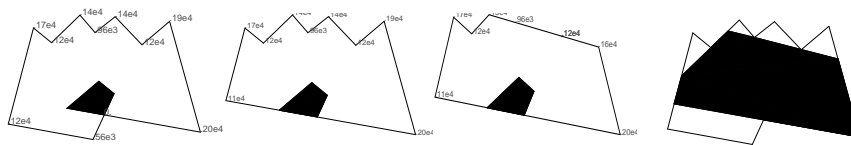


Figure 17. Some intermediate steps of the approximated MACS algorithm.

The figure 17 illustrates the intermediate steps of the approximated MACS algorithm and the figure 18 presents the result of the proposed algorithm on different shapes.



## References

- [1] A. Aggarwal, L. J. Guibas, J. Saxe, and P. W. Shor. A linear time algorithm for computing the Voronoi diagram of a convex polygon. In *Proceedings of the Nineteenth Annual ACM Symposium on Theory of Computing*, pages 39–45, New York City, 25–27 May 1987.
- [2] C. Andjar, C. Saona-Vzquez, and I. Navazo. LOD visibility culling and occluder synthesis. *Computer Aided Design*, 32(13):773–783, November 2000.
- [3] J. S. Chang and C. K. Yap. A polynomial solution for the potato-peeling problem. *Discrete & Computational Geometry*, 1:155–182, 1986.
- [4] J.M. Chassery. Discrete and computational geometry approaches applied to a problem of figure approximation. In *Proc. 6th Scandinavian Conf on Image Analysis (SCIA 89)*, pages 856–859, Oulu City, 19–22 1989.
- [5] K. Daniels, V. Milenkovic, and D. yRoth. Finding the largest area axis-parallel rectangle in a polygon. *Computational Geometry: Theory and Applications*, 7:125–148, 1997.
- [6] H. Edelsbrunner. Computing the extreme distances between two convex polygons. *Journal of Algorithms*, 6:213–224, 1985.
- [7] J. E. Goodman. On the largest convex polygon contained in a non-convex  $n$ -gon or how to peel a potato. *Geometricae Dedicata*, 11:99–106, 1981.
- [8] D. Roth K. Daniels, V. Milekovic. Finding the largest area axis-parallel rectangle in a polygon. *Comput. Geom. Theory Appl*, 7:125–148, 1997.
- [9] J. O’Rourke, A. Aggarwal, Sanjeev, R. Maddila, and M. Baldwin. An optimal algorithm for finding minimal enclosing triangles. *J. Algorithms*, 7(2):258–269, 1986.
- [10] Joseph O’Rourke. *Computational Geometry in C*. Cambridge University Press, 1993. ISBN 0-521-44034-3.
- [11] F. P. Preparata and M. I. Shamos. *Computational Geometry : An Introduction*. Springer-Verlag, 1985.
- [12] D. Wood and C. K. Yap. The orthogonal convex skull problem. *Discrete and Computational Geometry*, 3:349–365, 1988.